Available online at www.sciencedirect.com

SciVerse ScienceDirect

Procedia Engineering 58 (2013) 138 – 146

Procedia Engineering

www.elsevier.com/locate/procedia

The 12th Hypervelocity Impact Symposium

Modeling Experiments of Hypervelocity Penetration of Adobe by Spheres and Rods

Christopher S. Meyer*

U.S. Army Research Laboratory
RDRL-WML-H, Aberdeen Proving Ground, MD 21005-5066, USA

Abstract

The work described in this paper uses the Holmquist-Johnson-Cook equation of state and constitutive model for concrete and appropriate material parameters derived from mechanical test data to perform numerical simulations of penetration and perforation of adobe building material. Experimental results from the literature are modeled, and two-dimensional numerical simulations are carried out using the CTH Eulerian shock physics code. Two groups of simulations were performed in accordance with the experimental results. The first group is tungsten rod penetrators, with impact velocities ranging from 340 to 820 m/s, perforating adobe targets with thicknesses ranging from 71 to 497 mm, and comparison of the residual velocities predicted by the numerical simulations with the available experimental results. The second group is steel spheres, with impact velocities ranging from 500 to 3230 m/s, penetrating into adobe targets of semi-infinite thickness, and comparison of the depths of penetration predicted by the numerical simulations with the available experimental results. The technique described in this paper for modeling and simulation of adobe penetration and perforation is able to adequately predict the residual velocities and depths of penetration for the conditions modeled.

Selection and peer-review under responsibility of the Hypervelocity Impact Society

Keywords: numerical simulation; modeling; adobe; geomaterial; HJC; Holmquist Johnson Cook; Eulerian

1. Introduction

Numerical simulation of adobe building materials, which are primarily composed of clay and sand, is sparse in the literature, and little data is available on experiments or modeling penetration of these building materials. Early work has used the brittle failure kinetics (BFK) concrete material model [1] in continuum mechanics codes to simulate penetration of adobe building materials [2]. The BFK model is effective at predicting the peak load on a penetrator and so is useful for simulations involving penetrator design. Adobe was modeled in BFK simulations using default concrete material parameters but with the unconfined compressive strength (f'_c) adjusted to match adobe. The BFK model's strength in geomaterial penetration simulations for rapid design of penetrators lies in this capability to use the strength of a material without the need to determine parameters for the material. However, this method of modeling geomaterials' response to penetration does not capture the pressure-dependent strength behavior of the adobe itself because the material behavior is that of concrete scaled by a modified compressive strength input to match the material of interest. Figure 1 illustrates the difference in material response by presenting the uniaxial-strain behavior of several geomaterials including adobe, mortar, concrete, and brick [3–8]. Therefore, in response to a need for higher fidelity numerical simulations of adobe building

* Corresponding author. Tel.: 410-278-3803; fax: 410-278-3412.
E-mail address: christopher.s.meyer12.civ@mail.mil

doi:10.1016/j.proeng.2013.05.017

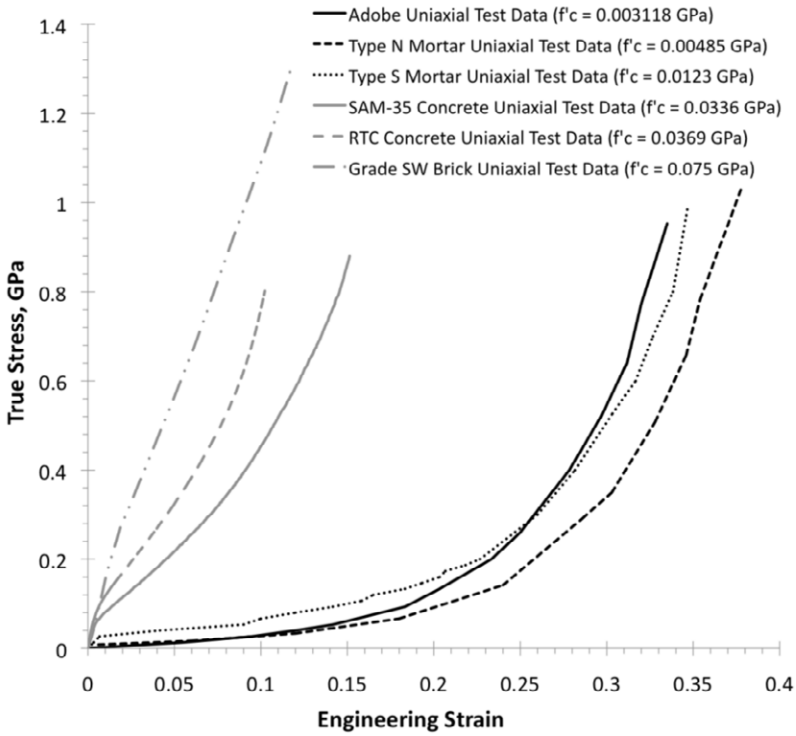

Fig. 1. Comparison of stress-strain behavior for various geomaterials showing the dissimilarity between adobe and concrete material behavior.

materials, it becomes necessary to establish material parameters for existing constitutive material models and, ultimately, develop material models that more precisely fit the material behavior.

In related work, the author began to establish a method for simulating the mechanical behavior of adobe [9]. This method is based on mechanical testing conducted by the U.S. Army Corps of Engineers Engineer Research and Development Center [3]. The numerical simulation of adobe uses the Holmquist-Johnson-Cook (HJC) constitutive model for concrete [10]. Many excellent constitutive models, including BFK, microplane model M4, and others, are available for numerical simulation of building materials. The HJC model was selected for this work because it expresses the pressure-dependent strength behavior of different geomaterials reasonably well, provides both an equation of state (EOS) and a material strength model, is readily available in many continuum mechanics codes, has a relatively low computational cost, the HJC model has previously been used to simulate high- and hypervelocity penetration of concrete [11], and importantly, material parameters are readily and straightforwardly derived from test data.

The present work utilizes the HJC model and adobe material parameters to simulate penetration and perforation of adobe at velocities ranging from 500 to 3230 m/s. Experimental results by Heine, Weber, and Wickert [12] for adobe penetration and perforation by a generic tungsten rod and steel spheres are modeled in this work. The resulting simulation results are compared to the reported experimental results. Simulation results evaluated include the predicted residual velocity (V_r) of rods after adobe target perforation and the predicted depth of penetration (DOP) of spheres into adobe. Note that experimental data on residual length of the penetrator rods were not available for comparison with numerical simulation results. Mathematical model results by Heine et al. [12] are examined in light of the simulation results, and the transition from rigid body to eroding penetration is discussed. The focus of this work is in establishing and beginning to validate, through comparison with available experimental data, a technique for numerical simulation of penetration and perforation of adobe building materials.

2. Problem setup

2.1. Target material

Heine et al. [12] reported two groups of yield strengths, Young's moduli, densities, and longitudinal sound velocities measured for the two groups of adobe target materials, one of which was perforated by rods and the other penetrated by spheres. The HJC adobe strength parameters that were previously derived from adobe mechanical characterization test data were adjusted according to the yield strengths and Young's moduli of the as-tested materials. The HJC adobe equation-of-state parameters used in these simulations included the densities and sound velocities as tested.

2.2. Rod model

In the tungsten rod perforation simulations, 90-mm-long rods, 6 mm in diameter (L/D=15) and with a 9-mm long cone chamfered down to a 3-mm-diameter blunt nose, were modeled. Note that Heine et al. [12] did not describe the exact specifications of the tungsten rods, but while there may be some geometry differences between the simulations and the as-tested conditions, the mass, 47 g, was equivalent. The primary focus of this work is to evaluate the adobe model and determine if it provides believable results and then determine its efficacy for use in future adobe penetration and perforation simulations. Tungsten was modeled using material parameters for a 93% tungsten, 5% nickel, 2% iron tungsten alloy [13] and the Mie-Grüneisen EOS, Johnson-Cook visco-plastic material strength and the Johnson-Cook fracture model. Simulations included rod penetration and perforation of monolithic adobe targets of the following thicknesses: 71, 142, 355, and 497 mm. Note that these thicknesses correspond to thicknesses outlined in [12] for a single adobe block (71 mm), two adobe blocks (142 mm), five adobe blocks (355 mm), and seven adobe blocks (497 mm); however, discrete blocks were not modeled. All simulations were two-dimensional (2-D) and were performed using the Eulerian shock physics code CTH [14], with adaptive mesh refinement and striking velocities ranging from 340 to 820 m/s.

2.3. Sphere model

Sphere penetration simulations included 13.5-mm and 10-mm-diameter steel spheres. 4340-steel was modeled with the Mie-Grüneisen EOS, Johnson-Cook visco-plastic strength and Johnson-Cook fracture models. Simulations were 2-D CTH [14] using adaptive mesh refinement and striking velocities ranging from 500 m/s to 3230 m/s. Heine et al. [12] described the target penetration as nondeforming. It is assumed in this work that this description implies rigid, noneroding penetration. Thus, steel spheres with a striking velocity near 2000 m/s were modeled first using default eroding, deforming material behavior and second with the Boundary Layer Interface (BLINT) technique described by Silling [15] and used by Scheffler [16, 17] for noneroding penetration simulations. The spheres were simulated penetrating into monolithic 355-mm-thick adobe, and boundary conditions were set to simulate semi-infinite target material.

3. Results and discussion

Table 1 reports the results of numerical simulation of perforation of adobe targets by high-velocity tungsten rods and compares these results with available experimental data. Tables 2 and 3 report the results of numerical simulation of penetration of adobe targets by high- and hypervelocity steel spheres of 13.5- and 10-mm diameters and compares these results with available experimental data. Figure 2 is an image from a 2-D simulation of the perforation of an adobe target by a generic tungsten rod with a length-to-diameter ratio of 15. Figure 3 shows a late-time penetration simulation image of a 13.5-mm diameter steel sphere into a semi-infinite adobe target. The simulations of high- and hypervelocity penetration of adobe by rods (reported in Table 1) and spheres (reported in Tables 2 & 3) predict residual velocities and DOPs reasonably well compared with the experimental results.

3.1. Rod residual velocity

The residual velocities predicted by the simulations for the various target thicknesses and impact velocities are plotted in Figure 4, with the model per equation (1) for the experimental data reported by Heine et al. [12]. It is apparent that the rod penetration simulation results are in family with the experimental results. Figure 4 plots residual velocity, V_r, calculated by Equation (1), with the constant, K = 9,729,000 g•m/s^2 as discussed by Heine et al. [12], mass, m = 47 g, and with initial velocity, V_0, and target thickness, x, as reported in Table 1. The goal of this work is not to evaluate the mathematical models or penetration results but merely to establish a technique for modeling and simulation of high-fidelity adobe

Table 1. Residual velocity (V_R) results for CTH simulations of L/D=15 tungsten rod perforation of adobe for various target thicknesses and impact velocities. Experimental results from Heine et al. [12].

Target Thickness (cm)	V_0 (m/s)	Experiment V_R (m/s)	Simulation V_R (m/s)	Simulation V_R Error (%)
7.1	510	480	492	2.5
7.1	810	790	795	0.6
14.2	330	280	270	3.6
14.2	350	280	299	6.8
14.2	410	340	375	10.3
14.2	460	390	426	9.2
14.2	490	420	447	6.4
14.2	820	780	785	0.6
35.5	460	270	321	18.9
35.5	480	300	346	15.3
35.5	540	370	416	12.4
35.5	710	580	603	4.0
35.5	800	680	709	4.3
49.7	810	630	680	7.9

Table 2. DOP results for CTH simulations of steel spheres penetrating into semi-infinite adobe for various impact velocities and sphere diameters. Experimental results from Heine et al. [12].

Sphere Diameter (mm)	V_0 (m/s)	Experiment DOP (cm)	Simulation DOP (cm)	Simulation Error (%)
13.5	610	6.1	8.8	44.3
13.5	900	9.0	11.7	30.0
13.5	1200	12.9	13.6	5.4
13.5	1460	12.5	13.3	6.4
13.5	1510	15.7	13.1	16.6
13.5	1950	13.1	8.9	32.1
13.5	2040	12.5	10.2	18.4
10	3230	6.7	6.8	1.5

Table 3. DOP results for CTH simulations using BLINT for steel spheres penetrating into semi-infinite adobe for various impact velocities and sphere diameters. Experimental results from Heine et al. [12].

Sphere Diameter (mm)	V_0 (m/s)	Experiment DOP (cm)	Simulation DOP (cm)	Simulation Error (%)
13.5	1200	12.9	13.2	2.3
13.5	1460	12.5	14.2	13.6
13.5	1510	15.7	14.2	9.6
13.5	1950	13.1	10.2	22.1
13.5	2040	12.5	10.3	17.6
10	3230	6.7	6.9	3.0

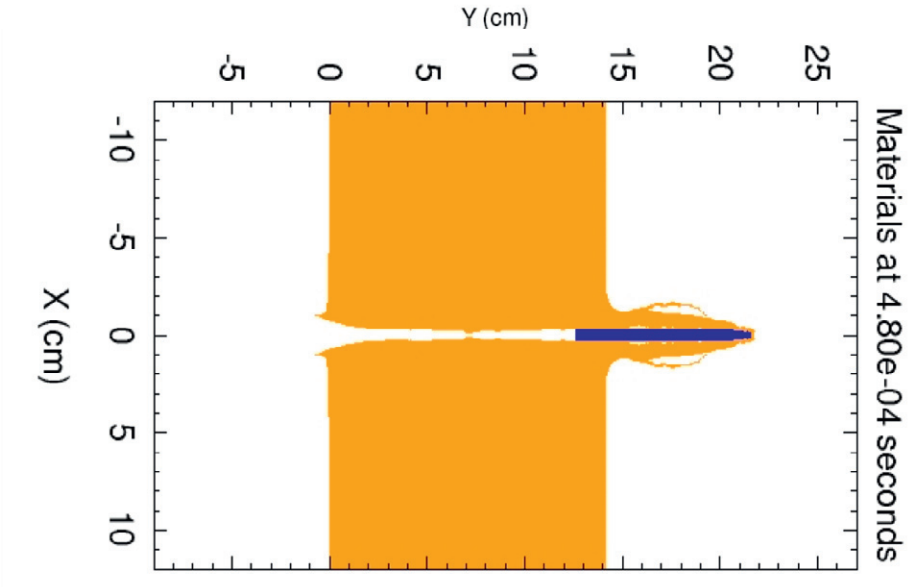

Figure 2. Two-dimensional CTH simulation of tungsten rod (V0 = 477 m/s) penetration and perforation through 142-mm adobe target.

Figure 3. Steel sphere penetration into semi-infinite adobe target (V_0 = 1200 m/s). (Note that penetration depth results from 2-D CTH simulations only are reported in this paper. A three-dimensional simulation image is shown here because it better illustrates the plastic deformation of the sphere, which is more difficult to visualize from the 2-D results.)

penetration and perforation and evaluate this technique on the basis of its capability to predict experimental results. Examining the error reported in Table 1 it is apparent that the method of simulating adobe perforation by tungsten rods described in this paper predicts residual velocity generally within about 10% of the experimental results. This method provides more accurate results for higher impact velocities, particularly in excess of about 500 m/s. Striking velocities around 500 m/s on the 35.5-cm-thick target produced less accurate results than seen overall, possibly since the calculation might not be capturing the proper state of eroding penetration occurring for these velocities and target thickness.

$$V_r = \sqrt{V_0^2 - 2 \cdot \frac{K}{m} \cdot x} \,. \tag{1}$$

3.2. Sphere penetration depth

DOP of the sphere experiments [12] and DOPs predicted in the simulations, both normalized by penetrator density and diameter, are plotted in Figure 5 versus the initial velocity. Figure 5 also includes a relationship per Heine et al. [12] for impact velocities below 1500 m/s. The numerical simulations of spheres penetrating into semi-infinite adobe predict DOP for the investigated conditions reasonably well, though in general the DOP results are not as accurate as the residual velocity results from rod perforation simulations. Large error is seen for simulation results below 1200 m/s and for results

approaching 2000 m/s, but experimental data is insufficient to know the scatter of possible DOP results for various striking velocities and, considering for example the experimental results for striking velocities of 1460 and 1510 m/s, it is possible that the simulation results remain consistent with the experimental results. Discussed later, mixed cell treatment and erosion are likely contributors to numerical simulation error. Additional experimental data and further numerical simulation work is needed to fully qualify the DOP prediction capability of the technique explored here. A linear relationship between penetration depth and impact velocity is described by Equation (2), where P is penetration depth, D is projectile diameter, ρ_P is the penetrator material density (in this case, 7.85 g/cm^3), ρ_T is target material density (in this case, 1.8 g/cm^3), A is a constant found in accordance with Heine et al. [12] to be 7.407 cm^2•s/g, and v_0 is the impact velocity of the projectile.

$$\frac{P}{D}\cdot\frac{1}{\rho_P}=\frac{4}{3\cdot\rho_T\cdot A}v_0\,. \tag{2}$$

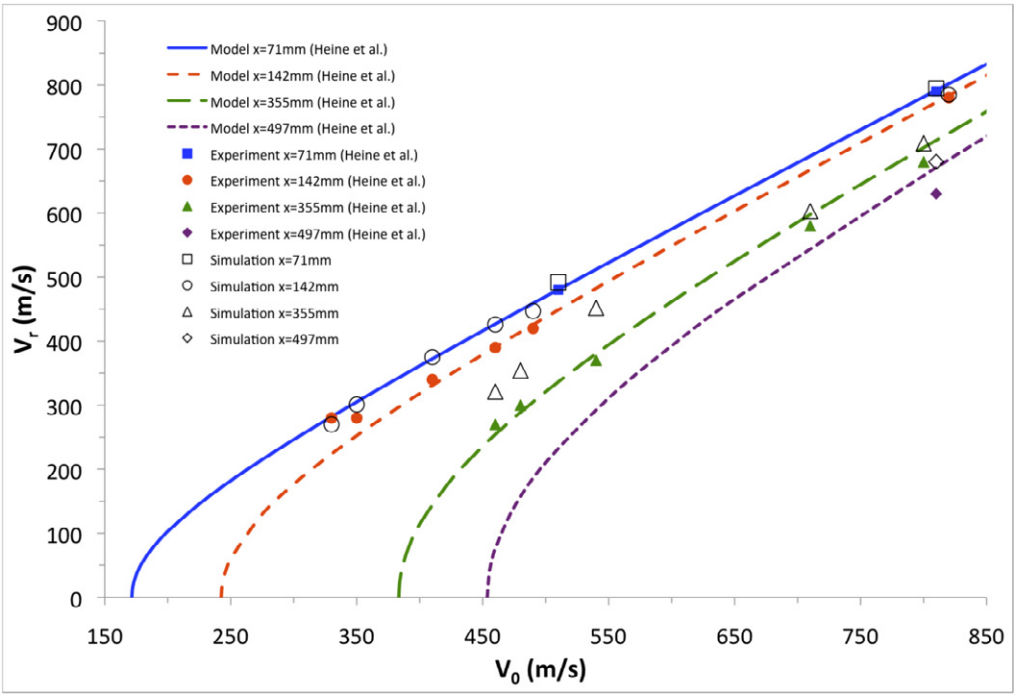

Figure 4. Comparison of tungsten rod penetration and perforation of adobe targets of indicated thicknesses. Results from experiments by Heine et al. [12] and CTH numerical simulations.

Penetration depth for both experimental and numerical simulation results increases in a linear fashion, with increasing impact velocity up to an apparent limiting velocity, after which the linear relationship between penetration depth and impact velocity breaks down. Simulation results begin to saturate above 1000 m/s, with a peak penetration depth occurring at a striking velocity of approximately 1300 m/s. Penetrator erosion and deformation are likely causes of the apparent drop in penetration depth with increasing penetrator velocity. Heider and Salk [18] report that for experiments and simulations of a steel rod impacting concrete, there is a transition regime from noneroding to eroding penetration in the velocity range from 1000 to 1200 m/s. Concrete is stronger and denser than adobe, but it is reasonable to expect these geomaterials to behave similarly in response to penetration by a much higher density projectile. The pressure-dependent strength of geomaterials may also contribute to the DOP in as yet undetermined ways. Geomaterials transition through three different phases. First, an elastic phase, which is infinitesimal compared to pressures applied during penetration; second, a crushing phase of microcracking and void collapse; finally, a fully compacted state in which a geomaterial like adobe is capable of being shocked. It is this shockable state that is of interest in penetration simulations, but material strength is a function of confining pressure in this state.

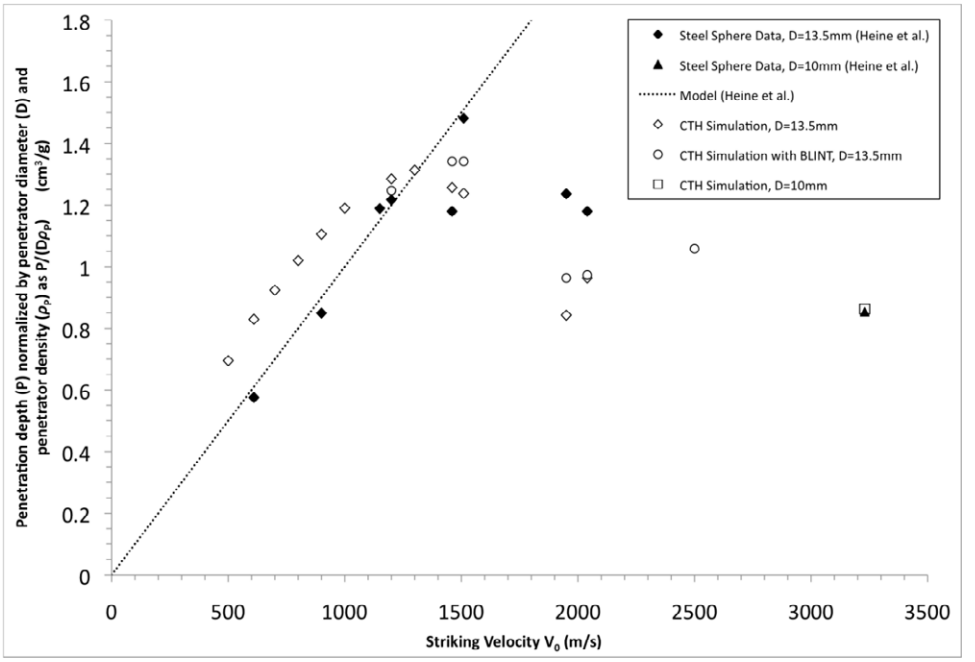

Figure 5. Comparison of steel sphere penetration depth, normalized by diameter and density, into semi-infinite adobe. Experiments by Heine et al. [12] and CTH numerical simulations.

Heider and Salk [18] performed calculations with the Tate-Alekseevskii model [19, 20] for penetration of a high-density, high-strength penetrator into a low-density, low-strength target. Similar to the results shown in Figure 5, Heider and Salk [18] found a drop in penetration depth with a transition from noneroding penetration (impact velocity near 1000 m/s) to penetration dominated by erosion (impact velocity approaching 2000 m/s). For impact velocities in excess of 2000 m/s, penetration depth is governed by the hydrodynamic limit, a function of projectile and target densities and sound velocities. It is well documented that a similar transition is seen between 1000 and 2000 m/s in the penetration of steel projectiles into aluminum targets [21, 22]. Therefore, the saturation of penetration depth with increasing impact velocity (seen in Figure 5) corresponds to a transition region (beginning between 1200 and 1500 m/s and continuing to around 2000 m/s) from noneroding to eroding penetration.

3.3. BLINT simulations

A well-known characteristic of Eulerian codes, including CTH [14], is that the total stress tensor is decomposed into strength and pressure terms where a constitutive model provides the strength and the EOS governs the pressure. In geomaterials such as adobe, the strength of the material is pressure-dependent [9], and the HJC model provides both an EOS and a pressure-dependent strength model. But even under pressure, adobe remains much softer than the penetrator. It has been reported that CTH has difficulty modeling rigid body penetration by a hard penetrator into a soft target material as well as difficulty modeling the sliding between two material interfaces [17]. Unfortunately, both of these conditions are included in the CTH simulations performed here. To overcome these limitations, the BLINT algorithm [15] in CTH was employed in numerical simulations for impact velocities within and greater than the erosion transition regime just discussed. BLINT allows definition of a soft and hard material and then moves the slip layer from the mixed cells between hard and soft materials to within the softer material. This soft material slip layer then allows the harder material to penetrate as a rigid body. Both the boundary layer between hard and soft materials and the slip layer in the soft material were set to two cells thick. Additionally, BLINT allows definition of a dimensionless scalar friction coefficient between soft and hard materials; in these simulations, friction was set to 0.28 [23].

Sphere penetrations for impact velocities of 1200 m/s and greater were modeled using CTH with the BLINT algorithm as well as CTH without BLINT. The results of BLINT calculations are shown in Table 3. In general, CTH simulations using BLINT predicted higher penetration depths than simulations without BLINT. BLINT predictions were nearer to

experimental results than standard CTH, with the exception of those of approximately 1500 m/s impact velocity. The 1500 m/s anomaly is believed due to impact velocity being in a region in which the penetration behavior transitions from strength-dominated behavior to a hybrid strength-and-pressure-dominated behavior. However, both standard CTH and CTH with BLINT simulations provided reasonable predictions of the penetration depths for the greater than 1500 m/s impact velocities tested.

Interestingly, simulations at the striking velocity 3230 m/s predicted penetration depths very close to the experimental result using both CTH with and without BLINT. This result is due to the fact that in the hydrodynamic limit the penetration depth is density driven and not strength driven. Of course, BLINT is not expected to provide much improvement in prediction capability for hypervelocity impacts where the EOS governs the penetration calculation. This expectation is because BLINT is designed for rigid body penetration; beyond the transition to eroding penetration, the BLINT model is not necessary.

As discussed by Scheffler [16], the BLINT technique breaks down when strength alone dominates the material behavior since BLINT creates a layer of slip cells between the hard and soft materials and these slip cells have no strength. Since the slip cells posses no strength, BLINT is less useful when strength effects alone govern the penetration calculation, as is true with lower velocities. Considering that the projectiles simulated here are spheres, there is little strength-governed lateral loading on the projectile. Since the penetration of the leading hemispherical surface will be dominated by pressure, BLINT still provides a useful technique for these simulations for impact velocities of greater than 1500 m/s. Scheffler [17] reported that CTH did an "adequate job of predicting the threshold velocity at which hemi-nose penetrators transition from rigid body to eroding rods." Scheffler's work consisted of hemispherical and ogival nose tungsten rods into aluminum; however, the simulations conducted here for steel spheres into adobe appear to agree. That is, for the material models and conditions simulated, CTH seems to have done an adequate job of predicting the threshold velocity at which steel spheres transition from rigid body to eroding in adobe penetration.

4. Conclusions

This work provides a framework for future modeling and simulation of adobe penetration and perforation using the Holmquist-Johnson-Cook constitutive model and EOS with adobe material parameters. The numerical simulations performed in this work generally predicted residual velocities and penetration depths reasonably well when compared with experimental results.

CTH calculations for a tungsten rod perforating an adobe target simulated using the HJC model with adobe material parameters is able to predict residual velocity with reasonable accuracy for the conditions modeled. Striking velocities of less than about 500 m/s and target thicknesses of about 35.5-mm and greater reduce the accuracy of the predictions, possibly due to mixed cell effects within CTH. However, discounting those conditions, this technique is generally able to predict residual velocities to within about 10%.

The behavior of steel spheres into adobe follows the trend seen for other hard penetrators into soft targets; CTH simulations agree with the trends observed experimentally. Based on the results of these CTH simulations, the following observations are made.

Strength-governed penetration behavior dominates for steel spheres into an adobe target at impact velocities of up to approximately 1200–1500 m/s. For impact velocities less than 1200–1500 m/s, the penetration depth follows an approximately linear relationship with impact velocity, and minimal deformation is expected only at the higher velocities of this region. Eulerian simulations, such as CTH, for low-velocity impacts of steel spheres into adobe targets approximate the experimental results with a relatively large apparent error. Future work in this velocity regime should be conducted using rigid, noneroding Lagrangian or arbitrary Lagrangian-Eulerian penetration simulations such as with EPIC or ALE3D.

There is a transition region of penetration in which both strength (constitutive model) and density (EOS) dominate penetration; in this region, the penetration depth no longer follows the linear relationship to impact velocity but penetration depth saturates and may even begin to decrease with increasing impact velocity. Projectile deformation and erosion are expected in this transition region. This region appears to begin by 1500 m/s and end at an upper limit of about 2000 m/s. In this region, numerical simulations using CTH with the BLINT algorithm provide more accurate depth of penetration results compared with CTH without BLINT.

As impact velocity continues to increase beyond 2000 m/s, the penetration behavior becomes hydrodynamic and pressure and density dominate the eroding penetration of steel spheres into an adobe target. Deformation may become severe with flattening of the leading edge of the sphere and erosion of lateral surfaces. Hydrodynamic penetration of steel spheres into adobe targets at hypervelocity impact velocities are well suited to Eulerian calculations, and CTH with and without the BLINT algorithm is able to accurately predict depth of penetration for such impacts.

Acknowledgements

The author would like to thank Mr. Daniel R. Scheffler for helpful comments and suggestions regarding this paper, especially in the light of his own work. Additional thanks to Dr. Andreas Heine for discussions and information on the experiments carried out by him and his colleagues, Dr. Karl E. Webber and Dr. Matthias Wickert at the Fraunhofer Institute for High-Speed Dynamics at the Ernst-Mach-Institut. Without their experimental data, this work could not have been completed. Finally, special thanks to Ms. Maria K. Brady for her excellent editorial efforts on this paper.

References

[1] Silling, S. A., 1997. Brittle Failure Kinetics Model for Concrete. SAND97-0439C, Sandia National Laboratories, Albuquerque, NM.
[2] Volkmann, E., Moser, R., 2011. Private communication.
[3] Williams, E. M., Akers, S. A., Reed, P. A., 2008. Laboratory Characterization of Adobe. ERDC/GSL TR-08-11, U.S. Army Corps of Engineers Engineer Research and Development Center, Geotechnical and Structures Laboratory.
[4] Williams, E. M., Akers, S. A., Reed, P. A., 2009. Laboratory Characterization of Type N Mortar. ERDC/GSL TR-09-5, U.S. Army Corps of Engineers Engineer Research and Development Center, Geotechnical and Structures Laboratory.
[5] Williams, E. M., Akers, S. A., Reed, P. A., 2008. Laboratory Characterization of Type S Mortar. ERDC/GSL TR-08-10, U.S. Army Corps of Engineers Engineer Research and Development Center, Geotechnical and Structures Laboratory.
[6] Williams, E. M., Akers, S. A., Reed, P. A., 2006. Laboratory Characterization of SAM-35 Concrete. ERDC/GSL TR-06-15, U.S. Army Corps of Engineers Engineer Research and Development Center, Geotechnical and Structures Laboratory.
[7] RTC Concrete data provided by S. A. Akers, 2011. U.S. Army Corps of Engineers Engineer Research and Development Center, Geotechnical and Structures Laboratory.
[8] Williams, E. M., Akers, S. A., Reed, P. A., 2007. Laboratory Characterization of Solid Grade SW Brick. ERDC/GSL TR-07-24, U.S. Army Corps of Engineers Engineer Research and Development Center, Geotechnical and Structures Laboratory.
[9] Meyer, C. S., 2012. Numerical simulations of the mechanical behavior of adobe. Proceedings, SEM XII International Congress & Exposition on Experimental & Applied Mechanics, Costa Mesa, CA.
[10] Holmquist, T. J., Johnson, G. R., Cook, W. H., 1993. A computational constitutive model for concrete subjected to large strains, high strain rates, and high pressures. 14th International Symposium on Ballistics. Quebec, Canada, pp. 591-600.
[11] Dawson, A., Bless, S., Levinson, S., Pedersen, B., Satapathy, S., 2008. Hypervelocity Penetration of Concrete. International Journal of Impact Engineering 35, pp. 1484-1489.
[12] Heine, A., Weber, K. E., Wickert, M., 2011. Experimental investigation of the penetration and perforation of building materials by projectiles. Proceedings of the 26th International Symposium on Ballistics, Miami, FL.
[13] Weerasooriya, T., 1998. Deformation Behavior of 93W-5Ni-2Fe at Different Rates of Compression Loading and Temperatures. ARL-TR-1719, U.S. Army Research Laboratory, Aberdeen Proving Ground, MD.
[14] McGlaun, J. M., Thompson, S. L., Elrick, M. G., 1990. CTH: A Three-dimensional Shock Wave Physics Code. International Journal Impact Engineering 10, pp. 351-360.
[15] Silling, S. A., 1992. Eulerian Simulation of the Perforation of Aluminum Plates by Nondeforming Projectiles. Report No. SAND92-0493, Sandia National Laboratories, Albuquerque, NM.
[16] Scheffler, D. R., 2006. Modeling Non-Eroding Perforation of an Oblique Aluminum Target Using the Eulerian CTH Hydrocode. International Journal Impact Engineering 32, p. 461.
[17] Scheffler, D. R., 1996. CTH Hydrocode Predictions on the Effect of Rod Nose-Shape on the Velocity at Which Tungsten Alloy Rods Transition From Rigid Body to Eroding Penetrators When Impacting Thick Aluminum Targets. Structures Under Shock and Impact IV, Computational Mechanics, Inc., Billerica, MA.
[18] Heider, N., Salk, M., 2011. The erosion threshold for high velocity geo-penetrators. Proceedings of the 26th International Symposium on Ballistics, Miami, FL.
[19] Alekseevskii, V. P., 1966. Penetration of a Rod Into a Target at High Velocity. Combustion, Explosion and Shock Waves 2, pp. 63-66.
[20] Tate, A., 1967. A Theory for the Deceleration of Long Rods After Impact. Journal of Mechanics Physics Solids 15, p. 387.
[21] Forrestal, M. J., Piekutowski, A. J., 2000. Penetration Experiments With 6061-T6511 Aluminum Targets and Spherical-Nose Steel Projectiles at Striking Velocities Between 0.5 and 3.0 km/s. International Journal Impact Engineering 24, p. 57.
[22] Piekutowski, A. J., Forrestal, M. J., Poormon, K. L., Warren, T. L., 1999. Penetration of 6061-T6511 Aluminum Targets by Ogive-Nose Steel Projectiles With Striking Velocities Between 0.5 and 3.0 km/s. International Journal Impact Engineering 23(1), pp. 723-34.
[23] Raous, M., Karray, M. A., 2009. Model Coupling Friction and Adhesion for Steel-Concrete Interfaces. International Journal of Computer Applications in Technology 34(1), pp. 42-51.